1987

Studies of the manganese site of photosystem II by electron paramagnetic resonance spectroscopy

Julio C. de Paula
Haverford College

W. F. Beck

A. F. Miller

R. B. Wilson

J. Chem. Soc., Faraday Trans. 1, 1987, **83** (12), 3635–3651

Studies of the Manganese Site of Photosystem II by Electron Spin Resonance Spectroscopy

Julio C. de Paula, Warren F. Beck, Anne-Frances Miller, Robert B. Wilson and Gary W. Brudvig*

Department of Chemistry, Yale University, New Haven, Connecticut 06511, U.S.A.

The Mn-containing catalytic site for photosynthetic water oxidation undergoes changes in oxidation states during the catalytic cycle. One of these intermediates, the S_2 state, can be studied directly by e.s.r. at liquid-helium temperatures. Two distinct e.s.r. signals from the S_2 state are produced when dark-adapted Photosystem II membranes are illuminated in the 130–200 K range: a $g = 4.1$ signal or a signal centred at $g = 2.0$ with many hyperfine lines, referred to as the multiline e.s.r. signal. The yields and magnetic properties of these e.s.r. signals are found to depend on the temperature at which the S_2 state is formed and the choice of cryoprotectant (ethylene glycol or sucrose). The intensity of the $g = 4.1$ e.s.r. signal obeys the Curie law in the 4.0–20.0 K temperature range. The S_2-state multiline e.s.r. signal exhibits an intensity maximum at 7.0 K which is independent of microwave powers below 2 mW, if the samples contain 30% ethylene glycol. This non-Curie behaviour is not observed in samples containing 0.4 mol dm^{-3} sucrose. A model is presented in which the S_2 state e.s.r. signals arise from an exchange-coupled Mn tetramer, where both ferromagnetic and antiferromagnetic exchange occur. According to our model, the multiline e.s.r. signal observed in samples suspended in 30% ethylene glycol originates from the thermally populated first excited $s = 1/2$ state of the exchange-coupled Mn tetramer, whereas the $g = 4.1$ e.s.r. signal arises from the ground $s = 3/2$ state of the Mn tetramer in a configuration that makes the $s = 1/2$ state thermally inaccessible. The different behaviour of the S_2-state multiline e.s.r. signal in samples containing sucrose can be explained by a small conformational change of the Mn complex which alters the exchange couplings. In support of our assignment of the multiline e.s.r. signal, we present spectral simulations at S-, X- and Q-bands. The fits to the experimental spectra at X- and Q-bands are improved if a small degree of anisotropy is introduced in the g tensor of the Mn complex.

It is now generally accepted that photosynthetic water oxidation by Photosystem II (PSII) of green plants occurs at an Mn-containing catalytic site, the O_2-evolving centre (OEC), which can exist in five intermediate oxidation states known as S_i ($i = 0$–4) states [for recent reviews see ref. (1)–(3)].

E.s.r. spectroscopy has played an extremely important role in the determination of the structure of Mn in the OEC. The S_2 state can be observed directly by e.s.r. at liquid-helium temperature after illumination of the dark-stable S_1 state in spinach PSII preparations at 130–200 K. The S_2-state e.s.r. signal obtained after 130 K illumination of dark-adapted PSII membranes exhibits a single 320–360 G wide turning point at $g = 4.1$.[4,5] A second form of the S_2 state exhibits a multiline e.s.r. signal and can be generated at the expense of the '$g = 4.1$' form by each of three methods: incubation in the dark of 130 K illuminated samples at 200 K;[4] illumination of dark-adapted PSII membranes at 200 K;[6] or flashing dark-adapted samples once at room temperature.[7] The resulting S_2-state multiline e.s.r. signal is centred at $g = 2.0$ and exhibits at least 18 well resolved

Table 1. Relative yields (%) of the $g = 4.1$ and multiline e.s.r. signals in illuminated PSII membranes[a]

	30% ethylene glycol		0.4 mol dm^{-3} sucrose	
	$g = 4.1$ signal	multiline signal	$g = 4.1$ signal	multiline signal
130–135 K illumination	100	0	100	18
130–135 K illumination followed by 200 K dark incubation	0	60	70	60
200 K illumination	0–10	90–100	75	100
200 K illumination followed by 200 K dark incubation	0	100	75	100

[a] Percentage values do not reflect absolute spin concentrations; they are normalized with respect to the maximum intensity of each signal in each type of sample.

nuclear hyperfine lines that are spaced by *ca.* 85–90 G, as would be expected of an exchange-coupled, mixed-valence Mn complex.

The discovery of the S_2-state multiline e.s.r. signal[7] was significant because it provided the first direct spectroscopic probe of the Mn site of the OEC. Even though these early e.s.r. studies have been complemented by an increasing body of biochemical and spectroscopic data, the details of the structure of this Mn site are still a matter of controversy. The chemical analysis of chloroplast or PSII membrane preparations has indicated that four Mn ions per PSII are required for optimal O_2 evolution activity.[8,9] Therefore, it is relevant to ask whether the OEC is composed of two Mn dimers that are structurally and functionally distinct, as suggested by Kambara and Govindjee,[10] a Mn tetramer where all four ions interact magnetically[11,12] or a combination of an Mn dimer and Mn mononuclear centres.[13]

In this contribution, we present new results that extend our previous studies of the magnetic properties of the S_2 state.[12,14] These data support our earlier conclusion that the S_2 state of the OEC is composed of an exchange-coupled Mn tetramer.

Experimental

PSII membranes were prepared according to the method of Berthold *et al.*[15] with the modifications introduced by Beck *et al.*[16] All resuspension buffer solutions contained 30% ethylene glycol as a cryoprotectant, unless otherwise noted. Low-temperature illumination of PSII membranes (130–200 K) was performed as described by de Paula *et al.*[17] E.s.r. spectroscopy was performed on a JEOL ME-3X spectrometer equipped with an Oxford Instruments ESR-900 liquid-helium cryostat and interfaced to a DEC MINC-23 computer. The sample temperature was checked with a Lake Shore Cryotronics carbon-glass resistor inserted into an e.s.r. tube containing 30% ethylene glycol. All calculations were performed on a VAX 11/780 computer.

Results

Effect of Cryoprotectants on the S_2-State E.S.R. Spectra

In order to minimize the amount of damage due to freezing of PSII membranes, cryoprotectants are routinely added to the suspension buffers. Either ethylene glycol or sucrose have been widely used by researchers who perform e.s.r. studies on the Mn site

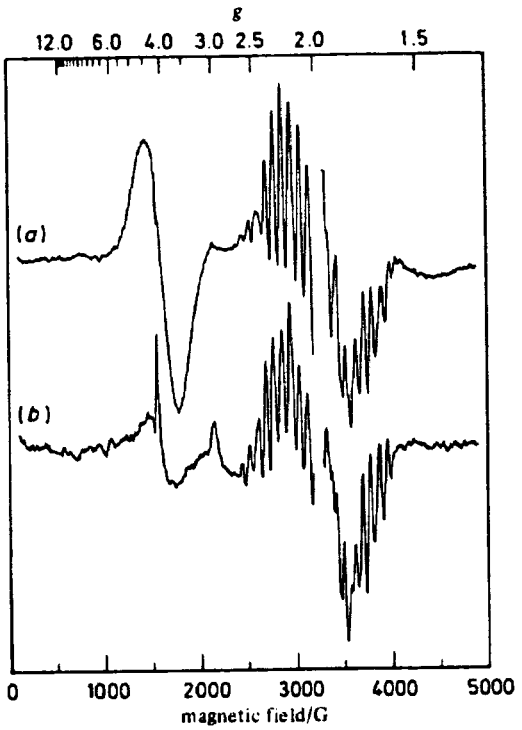

Fig. 1. Light-minus-dark difference e.s.r. spectra obtained by 200 K illumination of PSII membranes suspended in buffer solutions containing (*a*) 0.4 mol dm^{-3} sucrose or (*b*) 30% ethylene glycol. Instrument conditions: microwave power, 0.2 mW; modulation frequency, 100 kHz; modulation amplitude, 20 G; microwave frequency, 9.10 GHz; sample temperature, 7 K.

of the OEC at liquid-helium temperatures. It has been recently recognized, however, that the choice of cryoprotectant influences the e.s.r. spectra of the S_2 state.[18] As illustrated in fig. 1(*a*), illumination at 200 K of PSII membranes containing 0.4 mol dm^{-3} sucrose generates both the $g = 4.1$ and multiline e.s.r. signals. Furthermore, the amplitude of the $g = 4.1$ e.s.r. signal in these samples did not change appreciably upon incubation at 200 K in the dark for 2 min (table 1). In contrast, illumination at 200 K of PSII samples containing 30% ethylene glycol generates mostly the multiline e.s.r. signal [fig. 1(*b*)]. The small and variable amount of $g = 4.1$ e.s.r. signal obtained in these samples is completely converted to the multiline e.s.r. signal upon incubation at 200 K in the dark (table 1). Similar observations have led Zimmermann and Rutherford[18] to conclude that the S_2 state can be stably trapped at 200 K in two structurally distinct forms, one giving rise to the $g = 4.1$ e.s.r. signal and another giving rise to the multiline e.s.r. signal, if the suspensions contain sucrose. It is also apparent that the nuclear hyperfine interaction in the S_2-state multiline e.s.r. signal is slightly different in samples containing 0.4 mol dm^{-3} sucrose *vs.* 30% ethylene glycol, as judged by the intensity pattern of the hyperfine lines (fig. 1).

Kinetics of Conversion of the $g = 4.1$ E.S.R. Signal to the Multiline E.S.R. Signal

The $g = 4.1$ e.s.r. signal is generated by illumination at 130 K of PSII membranes containing ethylene glycol (table 1). This e.s.r. signal can be converted, however, to the multiline e.s.r. signal upon incubation in the dark at 200 K.[4] In order to gain more

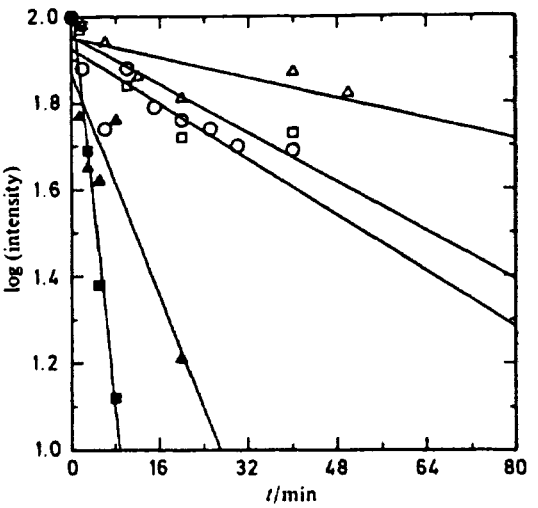

Fig. 2. Kinetics of conversion of the $g = 4.1$ e.s.r. signal to the multiline e.s.r. signal as probed by the disappearance of the $g = 4.1$ signal upon incubation in the dark at 140 K (△), 145 K (□), 150 K (○), 155 K (▲) and 160 K (■). Instrument conditions were as in fig. 1.

Table 2. Rate constants for the conversion of the $g = 4.1$ e.s.r. signal to the multiline e.s.r. signal

T/K	$k/10^{-4}$ s^{-1}
140	1.1
145	2.7
150	3.1
155	12.4
160	46.0

insight into the nature of this transition, its kinetics were investigated at several temperatures. The $g = 4.1$ e.s.r. signal was generated at 130 K, and then the sample was allowed to incubate in darkness at a given temperature for times ranging from 1 to 100 min. Consequently, kinetic traces were obtained between 140 and 160 K (fig. 2). The data could be fitted well with a single exponential decay of the $g = 4.1$ e.s.r. signal species in the dark at each temperature.

If we let P be the percentage of $g = 4.1$ e.s.r. signal remaining after incubation for a time t, then the rate equation becomes

$$\log P = -(k/2.303)t + \log P_0 \quad (1)$$

where k is the rate constant and P_0 is the percentage of $g = 4.1$ e.s.r. signal species present at $t = 0$, *i.e.* 100%. The lines drawn through the data in fig. 2 resulted from least-squares fits to eqn (1). The first-order rate constants are shown in table 2. Above 160 K the conversion of the $g = 4.1$ e.s.r. signal to the multiline e.s.r. signal was too rapid for an accurate measurement of the decay kinetics.

The data of table 2 can be rationalized in terms of the Arrhenius relation:

$$\log k = \log A - E_a/(2.303\,RT) \quad (2)$$

where A is the pre-exponential factor, E_a is the energy of activation for the process and R is the gas constant. A least-squares fit of the kinetic data to eqn (2) is shown in fig. 3.

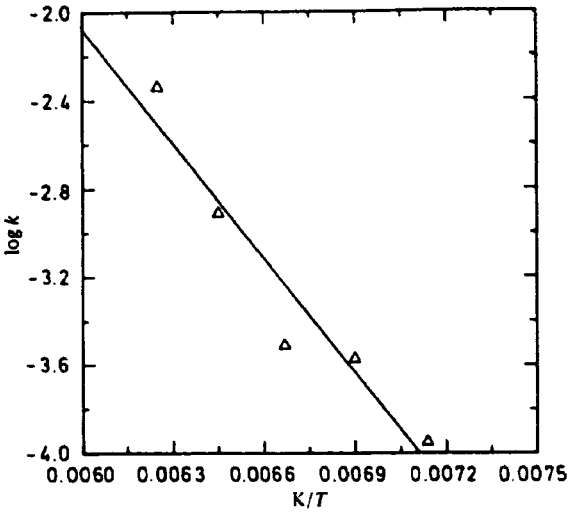

Fig. 3. Temperature dependence of the rate constants for conversion of the $g = 4.1$ e.s.r. signal to the multiline e.s.r. signal. The data in table 2 were fitted to the Arrhenius relation [eqn (2)]. The slope of the straight line plot is $-E_a/(2.303R) = -1726$ K and the y-intercept is $\log A = 8.28$. χ^2 for the fit was 0.040.

From that fit, an energy of activation of $E_a = 33 \pm 6$ kJ mol^{-1} and a pre-exponential factor of $A = (2.1 \pm 0.5) \times 10^8$ s^{-1} were obtained. From these parameters, the enthalpy and entropy of activation for the process at given temperatures can be calculated using

$$\Delta H^{\ddagger} = E_a - RT \qquad (3a)$$

$$\Delta S^{\ddagger} = R[\ln(Ah/kTe)] \qquad (3b)$$

where $\Delta H^{\ddagger}$ is the enthalpy of activation, $\Delta S^{\ddagger}$ is the entropy of activation, h is Planck's constant, k is Boltzmann's constant, and $e = 2.718$. At 140 K, $\Delta H^{\ddagger} = 32 \pm 6$ kJ mol^{-1} and $\Delta S^{\ddagger} = -88 \pm 36$ J mol^{-1} K^{-1}.

The results show that the entropy of activation for the conversion of the $g = 4.1$ e.s.r. signal species to the multiline e.s.r. signal species is negative. This implies the existence of a transition state that is more ordered than the initial state.

Temperature-dependence Studies

The temperature dependence of the e.s.r. signal from a polynuclear metal complex can be very diagnostic of the type of exchange interactions that exist between the metal centres. We have previously shown that the amplitude of the $g = 4.1$ e.s.r. signal increases with decreasing observation temperature over the temperature range 4–20 K.[12] This is an example of Curie law behaviour, which is expected from a transition within a ground-state spin level or a spin system in the high-temperature limit.

On the other hand, the S_2-state multiline e.s.r. signal exhibited an intensity maximum at $T = 7.0$ K.[12,14,15] Because an artifactual deviation from the Curie law can be observed if a saturating amount of microwave power is used to monitor the temperature dependence of the e.s.r. signal, it is important to ascertain that the temperature of the intensity maximum does not shift with varying microwave power. The data in fig. 4 clearly show that the temperature of the intensity maximum for the S_2-state multiline e.s.r. signal is not dependent on microwave power for powers of 2.6 mW or less. This result indicates that the S_2-state multiline e.s.r. signal arises from an excited-state spin manifold that becomes depopulated at $T < 7.0$ K.

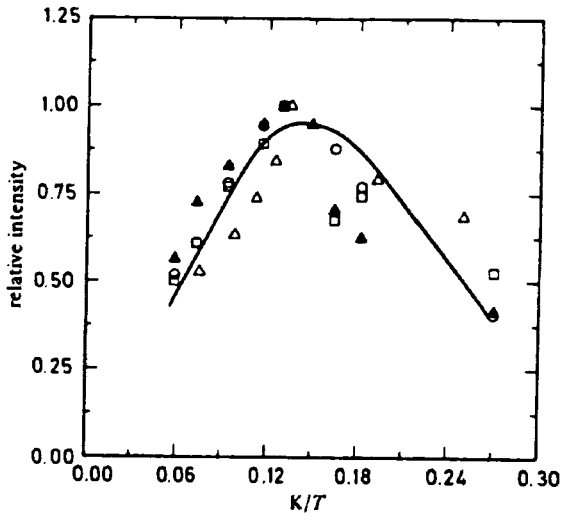

Fig. 4. The temperature dependence of the S_2-state multiline e.s.r. signal obtained by 200 K illumination of PSII membranes containing 30% ethylene glycol measured at several microwave powers. Spectrometer conditions as in fig. 1. ▲, 2.6 mW; ○, 0.2 mW; □, 0.02 mW; △, 0.006 mW.

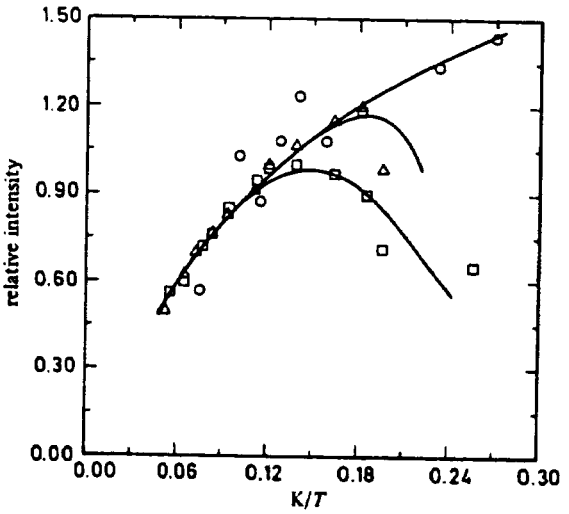

Fig. 5. Temperature dependence of the S_2-state multiline e.s.r. signal obtained in PSII membranes containing 0.4 mol dm^{-3} sucrose measured at several microwave powers. Spectrometer conditions as in fig. 1. □, 0.2 mW; △, 0.02 mW; ○, 0.006 mW.

Hansson *et al.*[20] have also studied the temperature dependence of the multiline e.s.r. signal generated by illuminating samples continuously while freezing to 77 K. They observed Curie behaviour in the range 3.7–6.3 K. It is noteworthy, however, that these researchers suspended their PSII membrane samples in buffer solutions containing 0.4 mol dm^{-3} sucrose, and not in 30% ethylene glycol. In order to test for the possibility that the choice of cryoprotectant may influence the results, we performed parallel studies in PSII membranes that were prepared as described above, except that 0.4 mol dm^{-3}

sucrose was substituted for 30% ethylene glycol throughout the isolation procedure. Fig. 5 shows that the S_2-state multiline e.s.r. signal from PSII membranes prepared in the presence of 0.4 mol dm^{-3} sucrose exhibits an intensity maximum which is dependent on the microwave power. Measurements made with the lowest microwave power approach the Curie law behaviour. The simplest conclusion to be drawn from these data is that the S_2-state multiline e.s.r. signal produced in samples suspended in buffer solutions containing 0.4 mol dm^{-3} sucrose arises from a ground state or low-lying level that is easily saturated. These results indicate that the structure of the Mn site in the S_2 state obtained by 200 K illumination is dependent on the medium in which the PSII membranes are suspended.

Discussion

A Theoretical Model of the S_2 State

It is believed that the S_2-state multiline e.s.r. signal arises from an $s = 1/2$ level, based on a g-value of *ca.* 2.0 for the e.s.r. signal and the lack of substantial g anisotropy.[13,21] Coupled with our results on samples containing 30% ethylene glycol, we conclude that the S_2-state multiline e.s.r. signal originates from a thermally excited $s = 1/2$ level of an Mn complex. The work of de Paula and Brudvig[14] has shown that the number of states below the e.s.r.-observable $s = 1/2$ state is on the order of 4, which is the degeneracy of an $s = 3/2$ state. Hence, in samples containing 30% ethylene glycol, the Mn complex in the S_2 state has an $s = 3/2$ ground state and a low-lying $s = 1/2$ first excited state.

A similarly unambiguous assignment of the S_2-state multiline e.s.r. signal from samples containing 0.4 mol dm^{-3} sucrose is not possible, however. This form of the S_2-state multiline e.s.r. signal apparently obeys the Curie law, thus suggesting that it arises from a ground-state spin manifold. On the other hand, because 3.7 K was the lowest observation temperature allowed by our set-up, we cannot dismiss the possibility that, in sucrose, the S_2-state multiline e.s.r. signal arises from an excited spin state that is depopulated at $T < 3.7$ K.

An assignment for the S_2-state $g = 4.1$ e.s.r. signal has been proposed by de Paula *et al.*[12] based on the following argument. It is known that the $g = 4.1$ and multiline e.s.r. signals both arise from Mn.[22] There is also substantial evidence that both e.s.r. signals arise from the same Mn complex.[17] A transition within the $m_s = \pm 1/2$ sublevels of an $s = 3/2$ state would appear at $g = 4.0$, provided that $|D| \gg h\nu$ and $|E| \approx 0$.[23] Also, the Curie temperature dependence of the $g = 4.1$ e.s.r. signal suggested that this signal arises from a ground-state level. Therefore, de Paula *et al.*[12] concluded that the $g = 4.1$ e.s.r. signal originates from the $s = 3/2$ ground state of the Mn complex in a configuration where the $s = 1/2$ excited state is thermally inaccessible. This assignment of the $g = 4.1$ e.s.r. signal to an $s = 3/2$ state ties in nicely with our assignment of the multiline e.s.r. signal. In both conformations of the Mn complex, the ground state has $s = 3/2$; the different forms only require a change in the splitting of the $s = 1/2$ and $s = 3/2$ states.

With these assignments in mind, we can begin to consider the structure of the Mn complex in the S_2 state. A dimer of Mn would be the simplest model for the S_2 state. Let us, then, consider a dimer of Mn^{III} ($s_1 = 2$) and Mn^{IV} ($s_2 = 3/2$). If these ions were coupled antiferromagnetically, then the ground and first excited spin states of the dimer would be $s = 1/2$ and $s = 3/2$, respectively. Although this coupling scheme provides the simplest explanation for the behaviour of the S_2-state mutliline e.s.r. signal in samples containing sucrose, it fails to account for the non-Curie temperature dependence of the S_2-state multiline e.s.r. signal when ethylene glycol was present. On the other hand, a ferromagnetically exchange-coupled Mn^{III}–Mn^{IV} dimer would have an $s = 7/2$ ground state, with the $s = 1/2$ state being the highest excited state of the complex. A manifold of 18 spin states lower in energy than the $s = 1/2$ state, as required for a

ferromagnetically coupled Mn^{III}–Mn^{IV} dimer, is also inconsistent with the temperature dependence of the S_2-state multiline e.s.r. signal observed in samples containing ethylene glycol.

It is clear, then, that a satisfactory explanation of our data can only be obtained if more than two Mn ions interact magnetically. There are currently three proposals for the involvement of four Mn ions in the structure of the OEC. Kambara and Govindjee[10] believe that Mn ions are arranged as two dimers that are structurally and functionally distinct. Hansson *et al.*[13] have proposed that the OEC is composed of a Mn dimer and two isolated Mn ions. A third view holds that four Mn ions interact to give a tetrameric structure.[11,12] Of these, only the Mn tetramer model can explain our data, as will be seen below.

The oxidation states of Mn in the OEC can be estimated from the X-ray absorption data of Goodin *et al.*[24] and the u.v. absorbance measurements of Dekker *et al.*[25] These studies suggest that both Mn^{III} and Mn^{IV} are present in the S_2 state of the OEC. There are, then, two equally reasonable combinations of oxidation states for an Mn tetramer in the S_2 state: $3Mn^{III}$–Mn^{IV} and $3Mn^{IV}$–Mn^{III}. Our e.s.r. spectral analyses cannot distinguish between these two cases. We have, therefore, considered both combinations of Mn oxidation states in the following calculations.

The zero-field spin Hamiltonian used to describe an exchange-coupled Mn tetramer is given by:

$$\hat{H}_{zf} = \sum_{i<k} J_{ik}\hat{s}_i\hat{s}_k + \sum_i D_i[\hat{s}_{iz}^2 - 1/3s_i(s_i+1)] \qquad (4)$$

where $\hat{s}_i$ and $\hat{s}_k$ are the electron spin operators, J_{ik} is the isotropic superexchange coupling constant between ions i and k, and D_i is the spin–spin coupling constant for each Mn ion. As we have written the superexchange Hamiltonian, $J_{ik} > 0$ for an antiferromagnetic interaction and $J_{ik} < 0$ for a ferromagnetic interaction.

A $3Mn^{III}$–Mn^{IV} Model

The zero-field Hamiltonian, $\hat{H}_{zf}$, for a $3Mn^{III}$–Mn^{IV} tetramer ($s_1 = s_2 = s_3 = 2$ and $s_4 = 3/2$) is described by a 500×500 matrix. As pointed out previously,[12] one of the requirements for obtaining an $s = 3/2$ ground state and an $s = 1/2$ first excited state with this model is that there be a strong antiferromagnetic exchange coupling between the Mn^{IV} ion and one of the Mn^{III} ions. This observation allows us to simplify the calculation because if we allow a dimer of Mn^{III}–Mn^{IV} to be very strongly antiferromagnetically exchange coupled, then only its $s = 1/2$ ground spin state need be considered when the weaker exchange couplings with the other two Mn^{III} ions are included. This reduces the problem to a trimer of $s_1 = s_2 = 2$ and $s_D = 1/2$, which can be described by a 50×50 Hamiltonian matrix, where s_D is the ground state of the antiferromagnetically exchange coupled Mn^{III}–Mn^{IV} dimer.

Further simplification can be achieved by letting $J' = J_{1D} = J_{2D}$ and $s' = s_1 + s_2$, where the coefficients 1, 2, and D refer to Mn ion 1 ($s_1 = 2$), Mn ion 2 ($s_2 = 2$), and the Mn^{III}–Mn^{IV} dimer ($s_D = 1/2$), respectively. If we let $J = J_{12}$ and $s = s' + s_D$, then the energy levels $E(s, s')$ are given by

$$\begin{aligned} E(s,s') &= \tfrac{1}{2}(J-J')[s'(s'+1) - s_1(s_1+1) - s_2(s_2+1)] \\ &\quad + \tfrac{1}{2}J'[s(s+1) - s_1(s_1+1) - s_2(s_2+1) - s_D(s_D+1)] \\ &= \tfrac{1}{2}(J-J')[s'(s'+1) - 12] + \tfrac{1}{2}J'[s(s+1) - 51/4]. \end{aligned} \qquad (5)$$

Fig. 6 gives a schematic representation of the exchange-coupling scheme used to arrive at the energies above and fig. 7 displays the energy levels $E(s, s')$ for several combinations of J and J'. It is clear that in order to obtain an ($s = 3/2$, $s' = 1$) ground state and an ($s = 1/2$, $s' = 0$) first excited state, J must be positive (antiferromagnetic exchange) and J' negative (ferromagnetic exchange). Furthermore, the following condition must apply:

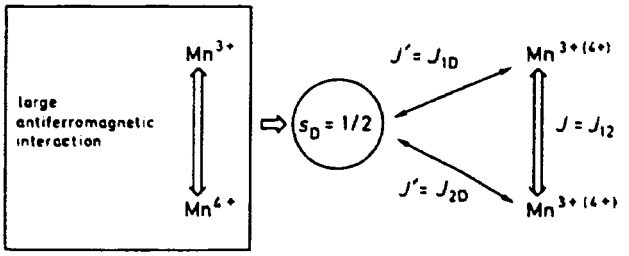

Fig. 6. Schematic representation of the exchange coupling scheme used in the simulation of the magnetic properties of the S_2 state. This diagram describes the notation and approximations used to calculate the zero-field energies of a $3Mn^{III}$–Mn^{IV} or $3Mn^{IV}$–Mn^{III} exchange-coupled tetramer.

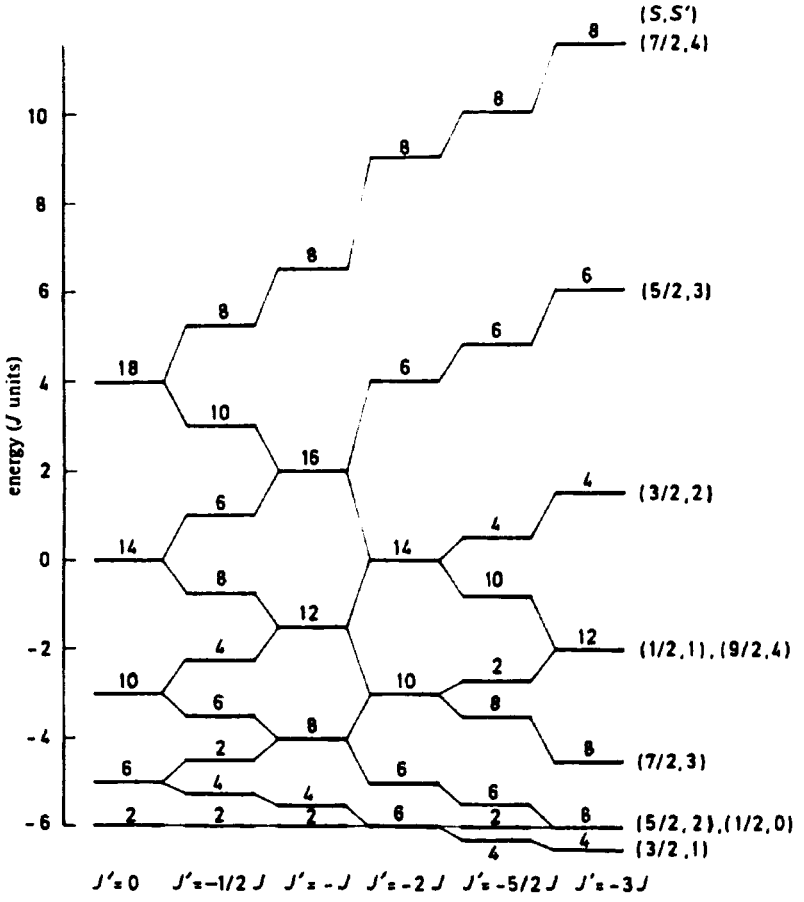

Fig. 7. Energy levels of a $3Mn^{III}$–Mn^{IV} exchange-coupled tetramer. The Hamiltonian is given by eqn (4) of the text and the energies are given in eqn (5). The number placed on top of each level denotes its degeneracy, given by $N_i = 2s_i + 1$.

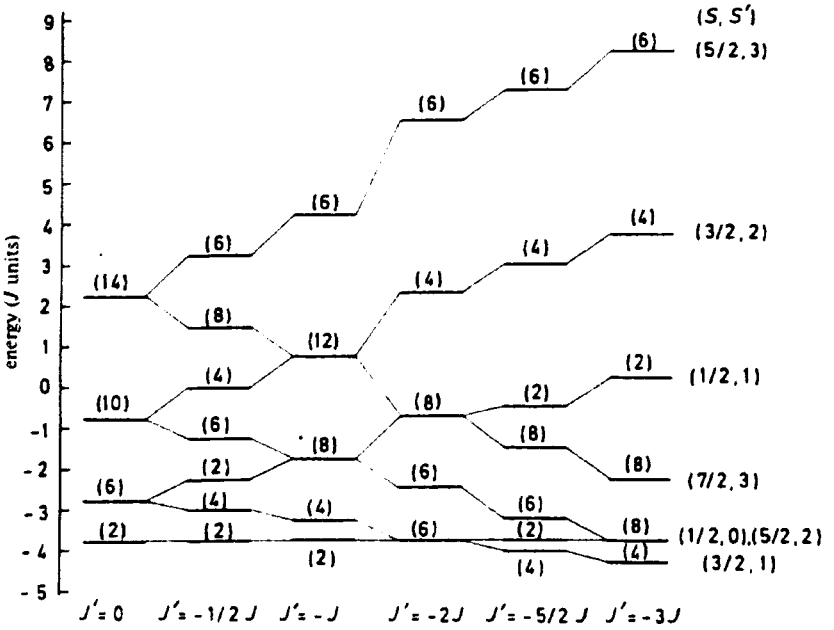

Fig. 8. Energy levels of a $3Mn^{IV}$–Mn^{III} exchange-coupled tetramer. The Hamiltonian is given by eqn (4) of the text and the energies are given in eqn (6). The number placed on top of each level denotes its degeneracy, given by $N_t = 2s_t + 1$.

$2|J| < |J'| < 3|J|$. Note that the antiferromagnetic exchange coupling between the Mn^{III}–Mn^{IV} pair must be large relative to either $|J|$ or $|J'|$ in this approximation.

A $3Mn^{IV}$–Mn^{III} Model

The ordering of the lower energy levels in a $3Mn^{IV}$–Mn^{III} tetramer that is exchange coupled as described in fig. 6 is qualitatively similar to the case described above for a $3Mn^{III}$–Mn^{IV} tetramer. In the case of a $3Mn^{IV}$–Mn^{III} tetramer, $s_1 = s_2 = 3/2$ and the energy levels $E(s, s')$ are given by

$$E(s, s') = \tfrac{1}{2}(J - J')[s'(s'+1) - 15/2] + \tfrac{1}{2}J'[s(s+1) - 33/4]. \quad (6)$$

Fig. 8 shows that a $3Mn^{IV}$–Mn^{III} tetramer will have a ground state of $s = 3/2$ and a first excited state of $s = 1/2$ only if $2|J| < |J'| < 3|J|$.

Assignments of the S_2-State E.S.R. Signals

We have proposed assignments for the S_2-state e.s.r. signals based on an exchange-coupled Mn tetramer.[12] These assignments were made by invoking the minimum variation in exchange couplings required to account for the temperature dependence of the e.s.r. signal intensities and, as shown below, the e.s.r. spectral properties (g values, ^{55}Mn nuclear hyperfine couplings) of the S_2 state.

The temperature dependence of the S_2-state multiline e.s.r. signal from samples containing ethylene glycol could be fitted satisfactorily using $J = 53.0\ cm^{-1}$, $J' = -120.0\ cm^{-1}$ and $D = -2.0\ cm^{-1}$.[12] The apparent Curie law behaviour of the S_2-state multiline e.s.r. signal from samples containing sucrose can be explained within the framework of this model in two ways. On the one hand, if $|J'| < 2|J|$, then the $s = 1/2$ level will be the

ground state of the Mn tetramer (see fig. 7 and 8) and the resulting e.s.r. signal would behave according to the Curie law. Consequently, a small decrease of *ca.* 20% in the ferromagnetic interaction between the Mn dimers is sufficient to account for the magnetic properties of the S_2-state multiline e.s.r. signal in samples containing sucrose. Alternatively, an even smaller decrease in the ferromagnetic interaction could bring the ground $s = 3/2$ state and the excited $s = 1/2$ state close enough together so that the temperature of an intensity maximum would be below 3.7 K, which is outside our range of detection. We note, however, that the S_2-state multiline e.s.r. signal in samples containing sucrose is extremely easily saturated (fig. 5). In view of past evidence that the Mn centre relaxes *via* an Orbach mechanism,[14,20,26] this result suggests that the S_2-state multiline e.s.r. signal in samples containing sucrose arises from a ground $s = 1/2$ state and that there are no low-lying excited states. This would correspond to the case where $|J'|$ is much smaller than $|J|$.

A good fit to the temperature dependence of the S_2-state $g = 4.1$ e.s.r. signal can be accomplished by invoking a transition within the $m_s = \pm 1/2$ levels of an $s = 3/2$ state, with the $s = 1/2$ state more than 15 cm^{-1} higher in energy, as proposed above. The combination of exchange couplings required for the fit is $J = 48.0\ cm^{-1}$, $J' = -130.0\ cm^{-1}$, and $D = 2.0\ cm^{-1}$ or $D = -1.0\ cm^{-1}$.[12]

Structure of the S_2 State

We can attempt to correlate the nature of the exchange interactions present in the Mn site with structure. It has been pointed out[12] that the pattern of exchange interactions in the Mn tetramer of the OEC, where both ferromagnetic and antiferromagnetic exchange occur, is analogous to that found in Cu_4O_4 cubane-like complexes[27] and the Fe_4S_4 centre of ferredoxin.[28] We proposed, therefore, that the Mn complex in the S_2 state has a Mn_4O_4 cubane-like structure.[12]

The assignment of the exchange coupling constants in the two forms of the S_2 state should also be considered together with the kinetic data for the conversion of the $g = 4.1$ e.s.r. signal to the multiline e.s.r. signal. It was determined above that the entropy of activation for the conversion of the $g = 4.1$ e.s.r. signal to the multiline e.s.r. signal is negative. The transition state, is therefore, more ordered than the '$g = 4.1$' conformation of the S_2 state. If we assume that the transition is endothermic, then we can invoke the Hammond postulate[29] and suggest that the S_2 state in the 'multiline' configuration, the final state, is more ordered than in the '$g = 4.1$' configuration, the initial state. This increase in order may be interpreted as a decrease in the number of degrees of freedom of the Mn tetramer within the protein matrix. Our simulations of the magnetic properties of the S_2 state in the '$g = 4.1$' and 'multiline' conformations provide complementary structural information. In order to fit the temperature dependence of the $g = 4.1$ e.s.r. signal it was necessary to decrease both J and J' relative to the values used to simulate the temperature dependence of the multiline e.s.r. signal. Extensive studies of exchange-coupled di-μ-hydroxo-bridged Cu^{II} dimers [reviewed in ref. (30)] have shown that the exchange interactions can range from strongly antiferromagnetic to strongly ferromagnetic as both the Cu—Cu distance and the Cu—O—Cu angle decrease. If we extend this view to the Mn complex in the S_2 state, then we can infer that some of the Mn—Mn distances and/or Mn—O—Mn angles have changed in going from the '$g = 4.1$' conformation to the 'multiline' conformation.

It is possible to consolidate the kinetic and magnetic data into a structural model for the conversion of the '$g = 4.1$' to the 'multiline' conformation. The decrease in the degrees of freedom of the tetramer can be taken as an indication that the Mn complex interacts strongly with the protein matrix in the 'multiline' conformation. On the other hand, the changes in Mn—Mn distances and Mn—O—Mn angles can result from changes in the environment of the bridging ligands. Perhaps a network of hydrogen

bonds to the bridging ligands is formed when the S_2 state is converted from the '$g = 4.1$' to the 'multiline' conformation. The formation of hydrogen bonds would certainly change the Mn—O—Mn angles and the Mn—Mn distances, as well as impart rigidity to the Mn tetramer, thereby leading to a more 'ordered' final state. Such hydrogen-bond networks have been proposed to exist in Fe_4S_4 centres of iron–sulphur proteins.[31]

There are alternative ways of interpreting our observations that the '$g = 4.1$' configuration of the S_2 state is less ordered than the 'multiline' form. It is possible that the increase in order may be related to a closer association of the Mn ions in the tetramer. This is in agreement with the proposal of Hansson *et al.*,[13] who have suggested that the $g = 4.1$ e.s.r. signal originates from an isolated Mn^{4+} ion.

Simulations of the S_2-State Multiline E.S.R. Signal

In an attempt to simulate the S_2-state multiline e.s.r. signal using a Mn tetramer model, we have determined the projection of the nuclear hyperfine coupling tensors of each individual ion on the total tetramer spin. It was found[12] that the multiline e.s.r. signal in ethylene glycol-containing samples has much Mn^{III}–Mn^{IV} dimer character (*i.e.* the second pair of Mn ions contribute only a very small nuclear hyperfine interaction), even though the explanation of the magnetic properties of the S_2 state requires a tetramer model. It should, then, be possible to obtain an approximate computer simulation of the S_2-state multiline e.s.r. signal with an antiferromagnetically exchange-coupled Mn^{III} ($s_1 = 2$)–Mn^{IV} ($s_2 = 3/2$) dimer as a model.

Our e.s.r. spectral simulations of the S_2-state multiline e.s.r. signal were performed in the coupled representation. If we let g_1, g_2, A_1' and A_2' be the single-ion g and A tensors, respectively, the dimer tensors g^c and A_i^c can be defined as

$$g^c = (1+C)/2\, g_1 + (1-C)/2\, g_2 \tag{7}$$

$$A_1^c = (1+C)/2\, A_1' \tag{8}$$

$$A_2^c = (1-C)/2\, A_2' \tag{9}$$

where
$$C = [s_1(s_1+1) - s_2(s_2+1)]/s(s+1). \tag{10}$$

The resonance condition is, then, given by:

$$h\nu = \beta HG + m_{I_1} A_1^c + m_{I_2} A_2^c + \{(A_1^c)^2[I_1(I_1+1) - m_{I_1}^2] + 1/4(A_2^c)^2[I_2(I_2+1) - m_{2I}^2]\}/\beta HG \tag{11}$$

where we have assumed isotropic nuclear hyperfine coupling constants for each Mn ion. The G term is a constant if the g tensor is isotropic; if an anisotropic g tensor is used in the calculation, G is written as

$$G = 2[(c_{1x} - 1/2\, c_{2x})^2 + 4(c_{1x}^2 - c_{1x} c_{2x} + c_{1y}^2 - c_{1y} c_{2y}) + c_{2x}^2 + c_{2y}^2]^{\frac{1}{2}} \tag{12}$$

where

$$c_{ix} = 1/2 g_{ix} \sin\theta \cos\phi \tag{13a}$$

$$c_{iy} = -1/2 g_{iy} \sin\theta \sin\phi \tag{13b}$$

$$c_{iz} = g_{iz} \cos\theta. \tag{13c}$$

The angles θ and ϕ define the direction of the magnetic field relative to the molecular principal axes. A computer program was written to simulate spectra for an Mn^{III}–Mn^{IV} dimer at S-, X- and Q-bands. The resonant field was determined using eqn (11) and a Gaussian lineshape was introduced at each resonant field position. The simulations in this paper required 30–40 increments of both θ and ϕ to achieve convergence.

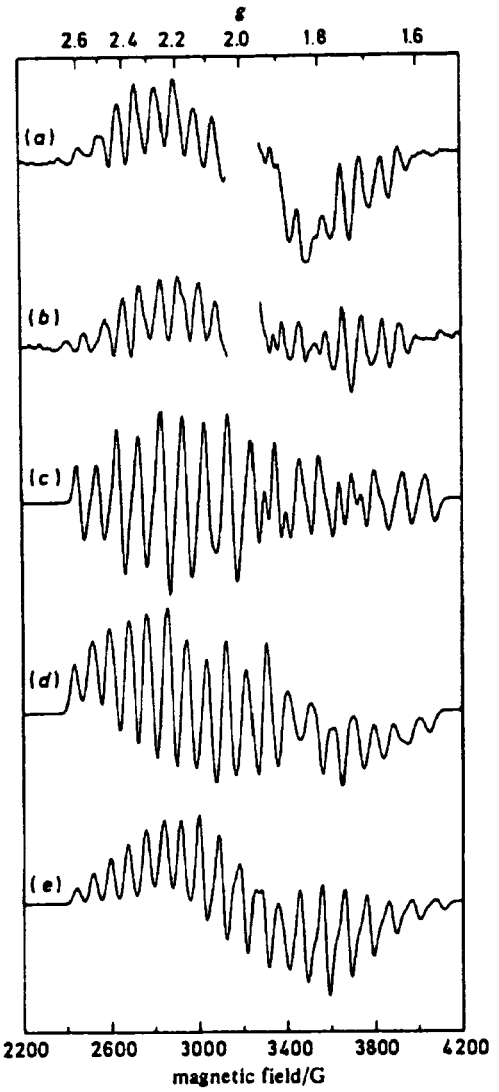

Fig. 9. Comparison between the experimental and calculated S_2-state multiline e.s.r. spectra at X-band ($\nu = 9.10$ GHz). Experimental spectra: (*a*) 200 K illuminated minus dark PSII; (*b*) 200 K illuminated then incubated at 0 °C for 1 min minus dark PSII treated with 250 μmol dm^{-3} DCBQ. Calculated spectra: (*c*) $g^c = 1.98$, $A_1^c = 0.0200\,\text{cm}^{-1}$, $A_2^c = -0.009\,30\,\text{cm}^{-1}$; (*d*) $g_x^c = 1.930$, $g_y^c = 2.0024$, $g_z^c = 2.100$, $A_1^c = 0.0170\,\text{cm}^{-1}$, $A_2^c = -0.0080\,\text{cm}^{-1}$; (*e*) $g_x^c = 1.810$, $g_y^c = 1.960$, $g_z^c = 2.274$, $A_1^c = 0.0086\,\text{cm}^{-1}$, $A_2^c = -0.0086\,\text{cm}^{-1}$.

An accurate evaluation of the lineshape of the S_2-state multiline e.s.r. signal is made difficult by the existence of other e.s.r. signals from PSII membranes in the 2200–4200 G region of the X-band spectrum. The e.s.r. signal II contribution at $g = 2.0$ cannot be easily subtracted out owing to the dynamic range of the digitization. There are, however, other sources of interference that can be eliminated. For example, difference spectroscopy subtracts away background contributions that are not light-induced. Also, de Paula *et al.*[12] have shown that the broad feature at $g = 1.9$ [fig. 9(*a*)], which is due

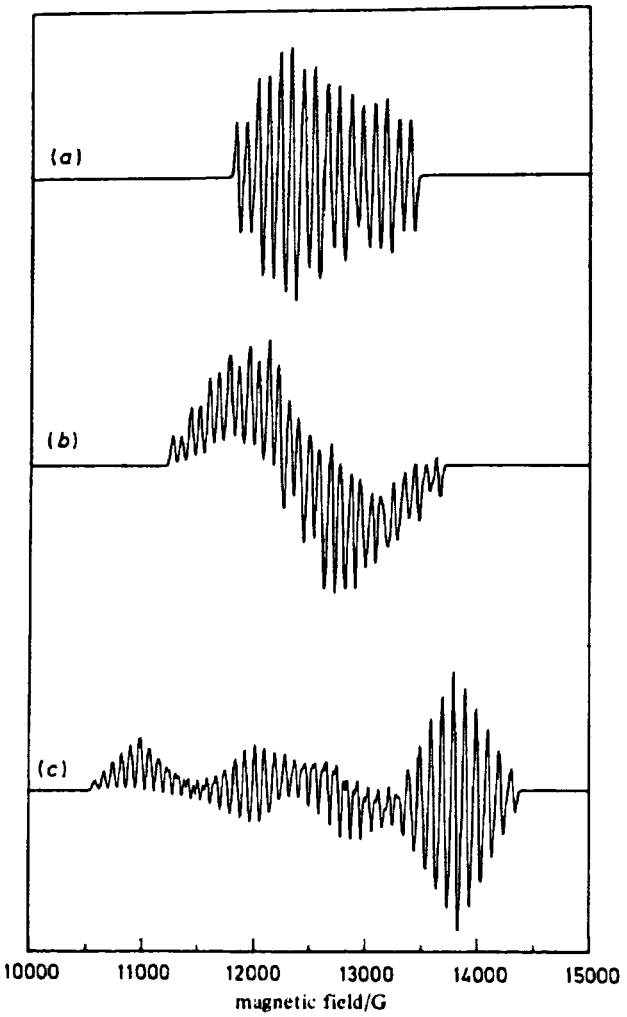

Fig. 10. Calculated S_2-state multiline e.s.r. spectra at Q-band ($\nu = 34$ GHz). (*a*) $g'_z = 1.98$, $A'_1 = 0.0200\ cm^{-1}$, $A'_2 = -0.00930\ cm^{-1}$; (*b*) $g'_x = 1.930$, $g'_y = 2.0024$, $g'_z = 2.100$, $A'_1 = 0.0170\ cm^{-1}$, $A'_2 = -0.0080\ cm^{-1}$; (*c*) $g'_x = 1.810$, $g'_y = 1.960$, $g'_z = 2.274$, $A'_1 = 0.0086\ cm^{-1}$, $A'_2 = -0.0086\ cm^{-1}$.

to the reduced electron acceptor Q_A, can be eliminated by reoxidation of Q_A^- with 2,5-dichloro-*p*-benzoquinone (DCBQ) following illumination [fig. 9(*b*)]. Therefore, our e.s.r. spectral simulations at X-band [fig. 9(*c*)–(*e*)] were optimized to reproduce the features of the spectrum in fig. 9(*b*). Fig. 9(*c*) shows a simulation that is analogous to that presented by Hansson and Andréasson.[26] It is seen that the use of an isotropic *g* value of 1.98 and inequivalent Mn ions fits the experimental spectrum poorly because the decrease in intensity observed in the low- and high-field extremes of the experimental spectrum is not reproduced in the calculation. Furthermore, the values of A'_i used to simulate the breadth of the e.s.r. spectrum are unreasonably larger than those expected for Mn^{III} or Mn^{IV}.[32]

In fig. 9(*d*), a small amount of *g*-anisotropy is introduced in the simulation. The values of A'_i were chosen to fall within the range expected for Mn^{III} and Mn^{IV}, *i.e.* $A'_i =$

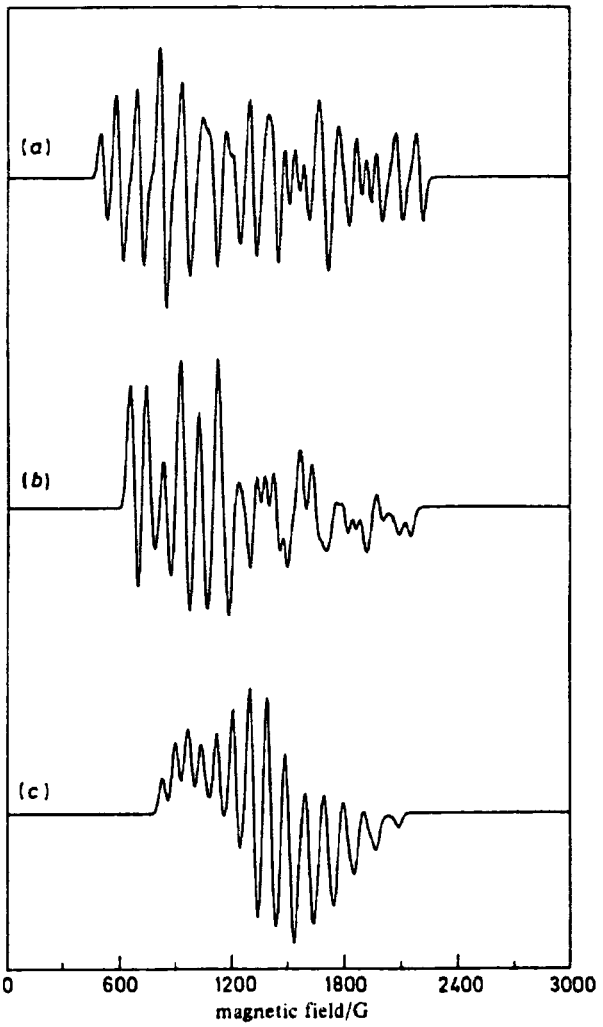

Fig. 11. Calculated S_2-state multiline e.s.r. spectra at S-band ($\nu = 4$ GHz). (*a*) $g^c = 1.98$, $A_1^c = 0.0200\ cm^{-1}$, $A_2^c = -0.00930\ cm^{-1}$; (*b*) $g_x^c = 1.930$, $g_y^c = 2.0024$, $g_z^c = 2.100$, $A_1^c = 0.0170\ cm^{-1}$, $A_2^c = -0.0080\ cm^{-1}$; (*c*) $g_x^c = 1.810$, $g_y^c = 1.960$, $g_z^c = 2.274$, $A_1^c = 0.0086\ cm^{-1}$, $A_2^c = -0.0086\ cm^{-1}$.

0.0070–$0.0090\ cm^{-1}$. The presence of g-anisotropy improved the quality of the fit over the isotropic case. The low-field portion of the experimental spectrum does not cross below the baseline, however, and this feature could not be reproduced in the calculations using a slightly anisotropic g tensor when the Mn ions are inequivalent. Fig. 9(*e*) shows a simulation of the S_2-state multiline e.s.r. signal where the degree of g-anisotropy is increased and the Mn ions are assumed to be equivalent, *i.e.* the values of A_i' were chosen so that $2|A_1^c| = |A_2^c|$. The positions and intensity pattern of the hyperfine lines to low field of $g = 2.0$ are more accurately reproduced in fig. 9(*e*), but it must be pointed out that their intensities are not well fitted in the high-field region of the spectrum.

It seems that the inclusion of anisotropy in the g tensor of an antiferromagnetically coupled Mn^{III}–Mn^{IV} dimer gives more accurate simulations of the S_2-state multiline e.s.r. signal [fig. 9(*d*) and (*e*)]. It is also necessary, however, to obtain experimental

verification for g anisotropy in the S_2-state multiline e.s.r. signal. Rutherford[21] has studied the S_2-state multiline e.s.r. signal obtained by 200 K illumination of PSII membranes and found that the lowest-field lines of the spectrum exhibit some orientation dependence. Indeed, our interpretation of the S_2-state multiline e.s.r. spectrum predicts that the lowest- and highest-field lines of the spectrum, which arise from g_z and g_x contributions, respectively, should exhibit the most accentuated orientation dependence. The lines closer to $g = 2.0$ have overlapping contributions from g_x, g_y and g_z which obscure the orientation dependence in this region.

Additional evidence for g anisotropy can come from the study of the S_2-state multiline e.s.r. signal at different microwave frequencies. Q-Band e.s.r. spectra of the S_2 state have been reported[13] whose nuclear hyperfine line spacings showed very few differences when compared to the X-band spectrum. Hansson *et al.*[13] also measured the magnetic field shifts for several of the hyperfine lines when the microwave frequency was varied from *ca.* 9.0 to 9.5 GHz. It was concluded that the multiline e.s.r. signal has a g value of 1.97 ± 0.04 and little or no g anisotropy.[13] Perhaps hyperfine rather than g anisotropy will be necessary to explain the lineshape of the Curie form of the multiline e.s.r. signal for which the varied frequency studies have been done. However, the extent of g anisotropy may be different in the non-Curie multiline e.s.r. signal or in the multiline e.s.r. signal in ammonia-treated samples.[16] Therefore, we have simulated Q-band (34 GHz) e.s.r. spectra of the S_2 state using the same simulation parameters as in the X-band spectra. The results are shown in fig. 10. It is observed that, in the case where g anisotropy is small, the S_2-state multiline e.s.r. signal is expected to show similar nuclear hyperfine structure at Q-band [fig. 10(*b*)] and X-band [fig. 9(*d*)]. The spacing between nuclear hyperfine lines is 88 and 94 G for the Q-band and X-band spectra, respectively. Furthermore, the two spectra differ only slightly in their overall width, with the Q-band spectrum extending over *ca.* 2500 G, whereas the X-band spectrum is 1700 G wide. However, in the case of larger g anisotropy [fig. 9(*e*) for X-band spectrum] the simulated Q-band multiline e.s.r. spectrum [fig. 10(*c*)] does deconvolute into its three g-value components and the spectral width changes from 1740 G at X-band to 3800 G at Q-band.

These preliminary simulations at Q-band show that perhaps measurements at a third frequency will be necessary to confirm the presence of g anisotropy in the S_2-state multiline e.s.r. signal. We are currently working towards obtaining e.s.r. spectra of the S_2 state at S-band. Even though we do not yet have data to report, our current model of the S_2 state predicts possible outcomes. Fig. 11 shows the results of our spectral simulations of the S_2-state multiline e.s.r. signal at S-band (4 GHz) with the same parameters used in fig. 9. It is interesting to note that, in the slightly anisotropic case [fig. 11(*b*)], the spectral width does not change significantly relative to the X-band spectrum, but the nuclear hyperfine structure shows destructive interference of the g_y and g_z turning points. We also observe that the inclusion of extensive anisotropy in the g-tensor gives an S-band spectrum whose width is only 1350 G (relative to 1740 G at X-band) with an envelope of nuclear hyperfine splittings that is strikingly similar to that of the X-band counterpart, but with fewer resolved lines [fig. 11(*c*)]. These results indicate that S-band e.s.r. will be very helpful in determining the extent of g-anisotropy in the S_2-state multiline e.s.r. signal.

We also expect to use S-band e.s.r. in an attempt to understand the nature of the $g = 4.1$ e.s.r. signal. We proposed above that the $g = 4.1$ e.s.r. signal originates from a transition within the $m_s = \pm 1/2$ levels of an $s = 3/2$ state. It is also possible, however, that the $g = 4.1$ e.s.r. signal could arise from a transition between the $m_s = \pm 1/2$ and $m_s = \pm 3/2$ sublevels of an $s = 3/2$ state, provided that $|D|$ is small. This assignment would require that $|D| \approx h\nu$ in order for a transition to be observed at $g = 4.1$ and also would make the effective g-value of the $g = 4.1$ signal dependent on the microwave frequency.

This research was supported by the National Institutes of Health (GM32715). G. W. B. is a Camille and Henry Dreyfus Teacher/Scholar (1985–90) and an Alfred P. Sloan Foundation Research Fellow (1986–88). W. F. B. is the recipient of a National Science Foundation Graduate Fellowship.

References

1 G. C. Dismukes, *Photochem. Photobiol.*, 1986, **43**, 99.
2 G. T. Babcock, in *New Comprehensive Biochemistry: Photosynthesis*, ed. J. Amesz (Elsevier, Amsterdam, in press).
3 G. W. Brudvig, *J. Bioenerg. Biomemb.*, 1987, **19**, 91.
4 J. L. Casey and K. Sauer, *Biochim. Biophys. Acta*, 1984, **767**, 21.
5 J-L. Zimmermann and A. W. Rutherford, *Biochemistry*, 1986, **25**, 4609.
6 G. W. Brudvig, J. L. Casey and K. Sauer, *Biochim. Biophys. Acta*, 1983, **723**, 361.
7 G. C. Dismukes and Y. Siderer, *Proc. Natl Acad. Sci. USA*, 1981, **78**, 724.
8 G. M. Cheniae, *Annu. Rev. Plant. Physiol.*, 1970, **21**, 467.
9 N. Murata, M. Miyao, T. Omata, H. Matsunami and T. Kuwabara, *Biochim. Biophys. Acta*, 1984, **765**, 363.
10 T. Kambara and Govindjee, *Proc. Natl Acad. Sci. USA*, 1985, **82**, 6119.
11 G. C. Dismukes, K. Ferris and P. Watnick, *Photobiochem. Photobiophys.*, 1982, **3**, 243.
12 J. C. de Paula, W. F. Beck and G. W. Brudvig, *J. Am. Chem. Soc.*, 1986, **108**, 4002.
13 Ö. Hansson, R. Aasa and T. Vänngård, *Biophys. J.*, 1987, **51**, 825.
14 J. C. de Paula and G. W. Brudvig, *J. Am. Chem. Soc.*, 1985, **107**, 2643.
15 D. A. Berthold, G. T. Babcock and C. F. Yocum, *FEBS Lett.*, 1981, **134**, 231.
16 W. F. Beck, J. C. de Paula and G. W. Brudvig, *Biochemistry*, 1985, **24**, 3035.
17 J. C. de Paula, J. B. Innes and G. W. Brudvig, *Biochemistry*, 1985, **24**, 8114.
18 J-L. Zimmerman and A. W. Rutherford, *Biochemistry*, 1986, **25**, 4609.
19 J. E. Sheats, B. C. UnniNair, V. Petrouleas, S. Artandi, R. S. Czernuszewicz and G. C. Dismukes, in *Progress in Photosynthesis Research*, ed. J. Biggins (Martinus Nijhoff, Dordrecht, 1987), vol. 1, p. 721.
20 Ö. Hansson, L-E. Andréasson and T. Vänngård, in *Advances in Photosynthesis Research*, ed. C. Sybesma (Nijhoff/Junk, The Hague, 1984), p. 307.
21 A. W. Rutherford, *Biochim. Biophys. Acta*, 1985, **807**, 189.
22 J. Cole, V. K. Yachandra, R. D. Guiles, A. E. McDermott, R. D. Britt, S. L. Dexheimer, K. Sauer and M. P. Klein, *Biochim. Biophys. Acta*, 1987, **890**, 395.
23 W. Weltner Jr, *Magnetic Atoms and Molecules* (Scientific and Academic Editions, New York, 1983), p. 241.
24 D. B. Goodin, V. K. Yachandra, R. D. Britt, K. Sauer and M. P. Klein, *Biochim. Biophys. Acta*, 1984, **767**, 209.
25 J. P. Dekker, H. J. van Gorkom, J. Wensink and L. Ouwehand, *Biochim. Biophys. Acta*, 1984, **767**, 1.
26 Ö. Hansson and L-E. Andréasson, *Biochim. Biophys. Acta*, 1982, **679**, 261.
27 W. Haase, L. Walz and F. Nepveu, in *The Coordination Chemistry of Metalloenzymes*, ed. I. Bertini, R. S. Drago and C. Luchinat (D. Reidel, Dordrecht, 1983), p. 229.
28 R. Cammack, D. P. E. Dickson and C. E. Johnson, in *Iron-Sulfur Proteins*, ed. W. Lovenberg (Academic Press, New York, 1977), vol. 3, p. 283.
29 G. S. Hammond, *J. Am. Chem. Soc.*, 1955, **77**, 334.
30 C. J. Cairns and D. H. Busch, *Coord. Chem. Rev.*, 1986, **69**, 1.
31 E. Adman, K. D. Watenpaugh and L. H. Jensen, *Proc. Natl Acad. Sci. USA*, 1975, **72**, 4854.
32 A. Abragam and B. Bleaney, *Electron Paramagnetic Resonance of Transition Ions* (Clarendon Press, Oxford, 1970).

Paper 7/665; *Received* 13*th April*, 1987